MITSUBISHI ELECTRIC RESEARCH LABORATORIES
http://www.merl.com

Mode-Evolution-Based Polarization Rotator-Splitter Design via Simple Fabrication Process

Yuan, W.; Kojima, K.; Wang, B.; Koike-Akino, T.; Parsons, K.; Nishikawa, S.; Yagyu, E

TR2012-006 April 2012

Abstract

A mode-evolution-based polarization rotator-splitter built on InP substrate is proposed by combining a mode converter and an adiabatic asymmetric Y-coupler. The mode converter, consisting of a bi-level taper and a width taper, effectively converts the fundamental TM mode into the second order TE mode without changing the polarization of the fundamental TE mode. The following adiabatic asymmetric Y-coupler splits the fundamental and the second order TE modes and also converts the second order TE mode into the fundamental TE mode. A shallow etched structure is proposed for the width taper to enhance the polarization conversion efficiency. The device has a total length of 1350 um, a polarization extinction ratio over 25 dB and an insertion loss below 0.5 dB both for TE and TM modes, over the wavelength range from 1528 to 1612 nm covering all C+L band. Because the device is designed based on mode evolution principle, it has a large fabrication tolerance. The insertion loss remains below 1dB and the polarization extinction ratio remains over 17dB with respect a width variation of +/-0.12 um at the wavelength of 1570 nm, or +/-0.08 um over the entire C+L band.

Optics Express

Mode-evolution-based polarization rotator-splitter design via simple fabrication process

Wangqing Yuan,[1,2] Keisuke Kojima,[1,*] Bingnan Wang,[1] Toshiaki Koike-Akino,[1] Kieran Parsons,[1] Satoshi Nishikawa,[3] and Eiji Yagyu[3]

[1]Mitsubishi Electric Research Laboratories, 201 Broadway, Cambridge MA, 02139, USA
[2]Departement of Electrical Engineering, Univeristy of Notre Dame, Notre Dame IN, 46556, USA
[3]Advanced Technology R&D Center, Mitsubishi Electric Corporation, 8-1-1 Tsukaguchi-Honmachi, Amagasaki, Hyogo 661-8661, Japan
[*]kojima@merl.com

Abstract: A mode-evolution-based polarization rotator-splitter built on InP substrate is proposed by combining a mode converter and an adiabatic asymmetric Y-coupler. The mode converter, consisting of a bi-level taper and a width taper, effectively converts the fundamental TM mode into the second order TE mode without changing the polarization of the fundamental TE mode. The following adiabatic asymmetric Y-coupler splits the fundamental and the second order TE modes and also converts the second order TE mode into the fundamental TE mode. A shallow etched structure is proposed for the width taper to enhance the polarization conversion efficiency. The device has a total length of 1350 μm, a polarization extinction ratio over 25 dB and an insertion loss below 0.5 dB both for TE and TM modes, over the wavelength range from 1528 to 1612 nm covering all C+L band. Because the device is designed based on mode evolution principle, it has a large fabrication tolerance. The insertion loss remains below 1 dB and the polarization extinction ratio remains over 17 dB with respect to a width variation of +/- 0.12 μm at the wavelength of 1570 nm, or +/- 0.08 μm over the entire C+L band.

OCIS codes: (130.0130) Integrated optics; (130.5440) Polarization-selective devices; (060.2340) Fiber optics components.

References and links

1. T. Barwicz, M. R. Watts, M. A. Popovic, P. T. Rakich, L. Socci, F. X. Kartner, E. P. Ippen, and H. I. Smith, "Polarization-transparent microphotonic devices in the strong confinement limit," Nat. Photonics **1,** 57-60 (2007).
2. L. M. Augustin, J. J. G. M. van der Tol, R. Hanfoug, W. J. M. de Laat, M. J. E. van de Moosdijk, P. W. L. van Dijk, Y. S. Oei, and M. K. Smit, "A single etch-step fabrication-tolerant polarization splitter," J. Lightwave Technol. **25,** 740-746 (2007).
3. H. Fukuda, K. Yamada, T. Tsuchizawa, T. Watanabe, H. Shinojima, and S. Itabashi, "Silicon photonic circuit with polarization diversity," Opt. Express **16,** 4872-4880 (2008).
4. W. Bogaerts, D. Taillaert, P. Dumon, D. V. Thourhout, R. Baets, and E. Pluk, "A polarization-diversity wavelength duplexer circuit in silicon-on-insulator photonic wires," Opt. Express **15,** 1567-1578 (2007).
5. R. Nagarajan, J. Rahn, M. Kato, J. Pleumeekers, D. Lambert, V. Lal, H. S. Tsai, A. Nilsson, A. Dentai, M. Kuntz, R. Malendevich, J. Tang, J. Zhang, T. Butrie, M. Raburn, B. Little, W. Chen, G. Goldfarb, V. Dominic, B. Taylor, M. Reffle, F. Kish, and D. Welch, "10 Channel, 45.6 Gb/s per channel, polarization-multiplexed DQPSK, InP receiver photonic integrated circuit," J. Lightwave Technol. **29,** 386-395 (2011).
6. M. R. Watts and H. A. Haus, "Integrated mode-evolution-based polarization rotators," Opt. Lett. **30,** 138-140 (2005).
7. M. R. Watts, H. A. Haus, and E. P. Ippen, "Integrated mode-evolution-based polarization splitter," Opt. Lett. **30,** 967-969 (2005).
8. J. Zhang, M. Yu, G. Lo, and D. Kwong, "Silicon-waveguide-based mode evolution polarization rotator," IEEE J. Sel. Top. Quantum Electron. **16,** 53-60 (2010).
9. L. Chen, C. R. Doerr, and Y. K. Chen, "Compact polarization rotator on silicon for polarization-diversified circuits," Opt. Lett. **36,** 469-471 (2011).

10. D. Dai and J. E. Bowers, "Novel concept for ultracompact polarization splitter-rotator based on silicon nanowires," Opt. Express **19,** 10940-10949 (2011).
11. K. Mertens, B. Scholl, and H. J. Schmitt, "New highly efficient polarization converters based on hybrid supermodes," J. Lightwave Technol. **13,** 2087-2092 (1995).
12. K. Mertens, B. Opitz, R. Hovel, K. Heime, and H. J. Schmitt, "First realized polarization converter based on hybrid supermodes," IEEE photonics technol. Lett. **10,** 388-390 (1998).
13. W. Burns and A. Milton, "Mode conversion in planar-dielectric separating waveguides," IEEE J. Quant. Electron. **11,** 32-39 (1975).
14. T. A. Ramadan, R. Scarmozzino, and R. M. Osgood Jr., "Adiabatic couplers: design rules and optimization," J. Lightwave Technol. **16,** 277-283 (1998).
15. Y. Shani, C. H. Henry, R. C. Kistler, R. F. Kazarinov, and K. J. Orlowsky, "Integrated optic adiabatic devices on silicon," IEEE J. Quant. Electron. **27**, 556-566 (1991).
16. T. Aalto, K. Solehmainen, M. Harjanne, M. Kapulainen, and P. Heimala, "Low-loss converters between optical silicon waveguides of different sizes and types," IEEE Photonics Technol. Lett. **18,** 709-711 (2006).
17. J. H. Schmid, B. Lamontagne, P. Cheben, A. Delage, S. Janz, A. Densmore, J. Lapointe, E. Post, P. Waldron, and D. -X. Xu, "Mode converters for coupling to high aspect ratio silicon-on-insulator channel waveguides," IEEE Photonics Technol. Lett. **19,** 855-857 (2007).
18. E. M. Garmire and H. Stoll, "Propagation losses in metal-film-substrate optical waveguides," IEEE J. Quant. Electron. 8, 763-766 (1972)
19. D. F. G. Gallagher and T. P. Felici, "Eigenmode expansion methods for simulation of optical propagation in photonics: pros and cons," Proc. SPIE **4987**, 69-82 (2003)
20. J. J. G. M. van der Tol, J. W. Pedersen, E. G. Metaal, Y. S. Oei, H. H. van Brug, and P. M. Demeester , "Adiabatic 3-db-coupler on InGaAsP/InP using double masking," Proc. SPIE **2449,** 349-354 (1995).
21. L. M. Augustin, R. Hanfoug, J. J. G. M. van der Tol, W. J. M. de Laat, and M. K. Smit, "A compact integrated polarization Splitter/converter in InGaAsP-InP," IEEE Photonics Technol. Lett. **19,** 1286-1288 (2007).

1. Introduction

Controlling polarization state of light in photonic integrated circuits (PICs) is of great importance for high-speed optical communication networks. First, the single mode fiber used in communication networks does not preserve the polarization state [1,2] and many components such as high index contrast waveguide [3] and micro-ring resonators [1] in PICs are polarization-sensitive. This polarization dependence along with the polarization mode dispersion degrades the performances of PICs at high modulation frequency. To solve the problem, polarization transparent systems were proposed [1,3,4]. Second, the polarization state can be utilized in polarization-division multiplexing (PDM) systems to double the spectral efficiency [5]. For the design of either the polarization transparent systems or the polarization multiplexing systems, the polarization manipulation devices including polarization rotator and splitter are key components.

The current designs of the polarization manipulation devices can be categorized into two types: mode coupling and mode evolution. The mode-coupling-based polarization manipulation devices, utilizing the mode beating behavior determined by device geometry and operating wavelength, are inherently fabrication sensitive and wavelength dependent. On the other hand, mode-evolution-based devices have relatively longer device length, required to achieve adiabatic transition, but larger bandwidth and better fabrication tolerance.

To take the benefit of the large bandwidth and fabrication tolerance, it is required to achieve a combination of polarization splitter and rotator both operating based on the mode-evolution principle. However, this combination is difficult to realize by a simple fabrication process. For example, to fabricate the design of the mode-evolution-based polarization splitter-rotator proposed by Watts *et al*. [1,6,7], a complicated process [6,8,9] including E-beam lithography was used to achieve the precise dimensional control of asymmetric bi-level tapers. This complicated process will reduce the manufacture yield and thus increase the cost per individual device. Alternative solutions include combinations of mode-evolution device (polarization splitter or rotator) and mode coupling device (polarization rotator or splitter) [10-12]. One solution [12] includes deep etched width taper, *i.e.*, mode-evolution device, connected to directional coupler, *i.e.*, mode-coupling device. Another solution [10,11]

includes a constant width waveguide, *i.e.*, a mode-coupling device connected to asymmetric Y-coupler, *i.e.*, mode-evolution device. As an advantage, such converters can have relatively small length. However, mode evolution device in series with mode coupling device do not preserve the benefits of using mode evolution device, such as large bandwidth and fabrication tolerance. Accordingly, there is a need to design a polarization rotator-splitter which has a large bandwidth and is simple in fabrication.

In this article, we propose a mode-evolution-based polarization rotator-splitter built on InP substrate, combining the adiabatic width taper with asymmetry Y-coupler [13,14]. Both devices are mode-evolution-based devices and easy to fabricate, resulting in large bandwidth and fabrication tolerance. This article is structured in two parts: first, the operation principle and structure design are introduced; then, the device performances over the C+L band and the performance variations with respect to fabrication errors are presented.

2. Principle and design

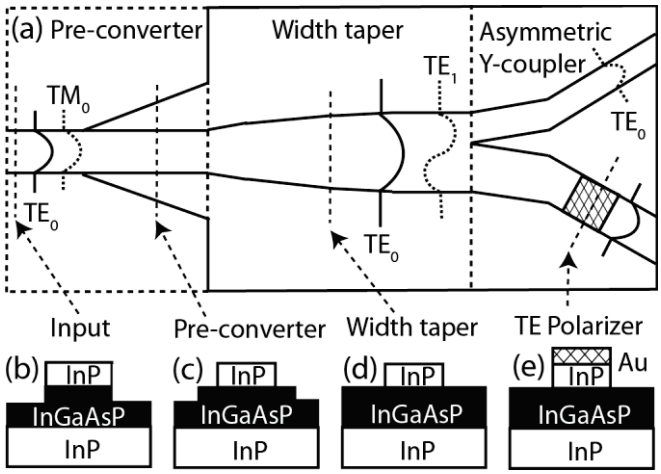

Fig. 1. The schematic top view (a) and cross section views (b)(c)(d)(e) of the proposed mode-evolution-based polarization rotator and splitter consisting of a pre-mode converter, a width taper, and an asymmetric Y coupler integrated with a TE mode polarizer.

A schematic diagram of the proposed mode-evolution-based polarization rotator-splitter is shown in Fig. 1(a). The device is designed for the InP/InGaAsP material system, consisting of InP substrate, 370 nm thick InGaAsP core layer with As composition of 60% lattice matched to InP, and 170 nm thick InP upper cladding layer. The device is composed of two parts, a mode converter and an asymmetric Y coupler.

The mode converter, consisting of a bi-level taper pre-converter and a width taper as shown in Fig. 1(a), is designed to transform the TM_0 mode to the TE_1 mode without changing TE_0 mode. To convert the TM_0 mode to TE_1 mode, the polarization is rotated by 90º. For the current design, approximately 95% of the 90º polarization rotation is realized in the width taper and the remaining 5% is realized in the pre-converter. The waveguiding structure of the width taper is designed by selectively etching through the InP upper cladding layer until reaching the InP/InGaAsP interface as shown in Fig. 1(d). Figure 2 shows the effective index of modes in this structure as a function of waveguide width. At the input of width taper with a width of 2 μm, the effective index of TM_0 mode is larger than that of TE_1 and the index difference is relatively large. As the waveguide width increases up to 2.6 μm, the index difference between the TE_1 and the TM_0 becomes smaller. Due to the structure asymmetry in vertical direction, these two modes interact with each other and form two hybrid modes, which are neither pure TE nor TM polarization. With the further increase of waveguide width beyond 2.6 μm, the index difference starts to increase and two hybrid modes evolves back into TE_1 and TM_0 modes respectively. It should be noted that at the output of the width taper

with a width of 3.1 μm, the second highest index mode (H_1) which is TM_0 mode at the input of the width taper becomes a TE_1 mode. Therefore, a TM_0 mode will be converted via the larger index hybrid mode into the TE_1 mode along width taper as shown by arrows in Fig. 2. Ideally, the polarization conversion efficiency (PCE) can be 100% for device with infinite length. However, for practical device with limited length, the PCE can never reach 100% and does depend on the effective index gap between two hybrid modes. According to the adiabatic criterion, both the coupling strength between two hybrid modes and the PCE increases with the increase of the gap size [15].

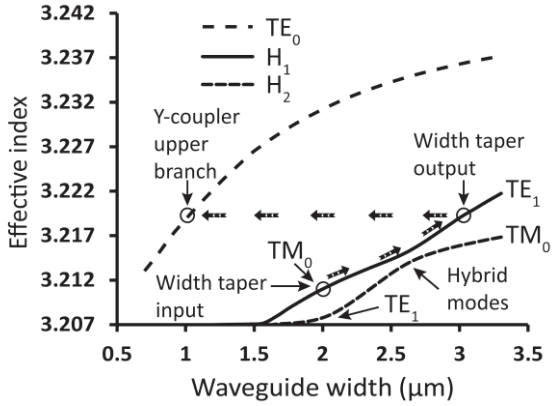

Fig. 2. The effective index of TE_0, the 2nd highest index mode, H_1, and the 3rd highest index mode, H_2, as a function of waveguide width at the wavelength of 1570 nm.

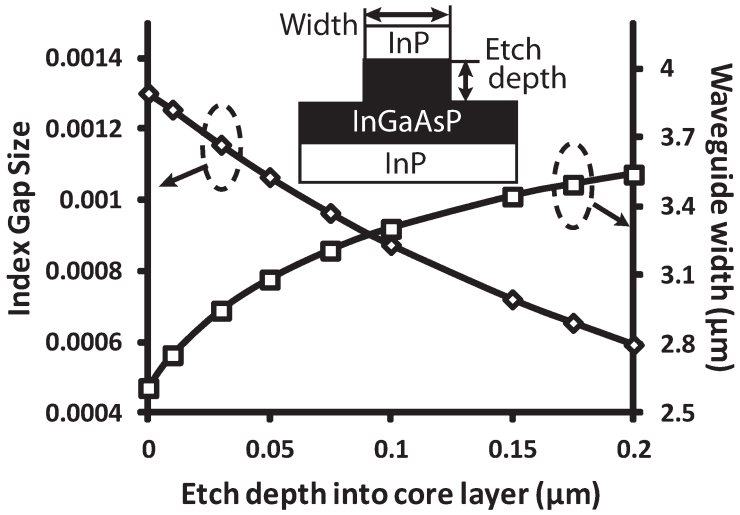

Fig. 3. The effective index gap between two hybrid modes with 50% TE and 50% TM polarization and the waveguide width as a function of etch depth into the InGaAsP layer (inset) at the wavelength of 1570 nm.

To obtain the optimal PCE for the width taper, the dependence of the effective index gap size on device geometrical parameter is investigated. Figure 3 shows the effective index gap between two hybrid modes with 50% TE and 50% TM polarization as a function of the etch depth into InGaAsP core layer at the wavelength of 1570 nm. Each waveguide width of the hybrid mode with 50% TE and 50% TM polarization has different values for each etch depth. These values are determined by parameter scanning and plotted in Figure 3. The hybrid modes with 50% TE and 50% TM polarization for each etch depth are determined by scanning the waveguide width. Figure 3 demonstrates that as the etch depth decreases, the effective index

gap increases, resulting in higher PCE. For this reason, the structure with zero etch depth into the InGaAsP layer is used in our design. However, the strong modes hybridization resulted from this structure causes problems. The H_1 mode at the input of this width taper is not pure TM_0 mode and contains about 5% TE polarization. A pre-converter has to be used to connect another waveguide with pure TM_0 mode to the input of width taper and also to convert the remaining 5% polarization. A waveguide with pure TM_0 mode can be realized by further etching the waveguide structure of the width taper into the InGaAsP core layer by 0.1 μm as shown in Fig. 1(b). An adiabatic bi-level etch-depth taper [16,17] shown in Fig. 1(c) can be used to realize the function of the pre-converter. To our knowledge, this is the first use of this type of taper for polarization conversion.

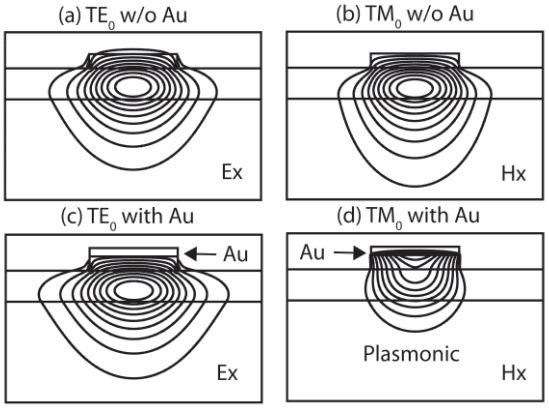

Fig. 4. Comparison of the mode field distributions with and without gold overlap. Electric field in horizontal direction, E_x, is plotted for TE_0 mode; magnetic field in horizontal direction, H_x, is plotted for TM_0 mode.

As shown in Fig. 1(a), the asymmetric Y-coupler [13,14] is designed to evolve the TE_1 and TE_0 from the output of the width taper into TE_0 in the upper branch and the TE_0 in the lower branch of Y-coupler, respectively. To realize these functions, the waveguide width in the upper branch of the Y-coupler is chosen so that the effective index of TE_0 in the upper branch of the Y-couple is equal to that of TE_1 at the output of width taper as illustrated in Fig.2. The asymmetric Y-coupler has very low insertion loss with high splitting ratio, which will contribute to improving the polarization extinction ratio (PER) for the polarization rotator-splitter.

If the PCE of the mode converter is not 100%, the unconverted TM_0 mode from the output of width taper will also evolve into the TM_0 mode in the lower branch, resulting in lower PER. To solve this problem, a TE mode polarizer integrated into the Y-coupler is proposed to filter out the TM_0 mode. The TE polarizer, similar to the device in [18], can be realized by simply depositing 100 nm gold on the top of the lower Y-branch waveguide. Figure 4 shows the comparison of mode field distribution of the TE_0 and TM_0 with and without gold overlayer. Compared with the propagation TM_0 modes without gold overlayer as shown in Fig. 4(c), the TM_0 mode with gold overlayer as shown in Fig. 4(d) becomes a plasmonic mode whereas the TE_0 mode remains a propagation mode after depositing gold overlayer. The absorption coefficient for the plasmonic TM mode is more than 100 times larger than that for the propagation TE mode as shown in Fig. 4(c). In addition, the transition loss between propagation TM mode and plasmonic TM mode is much larger due to the large mode mismatch as shown in Fig. 4. As a result, a TE polarizer with an extinction ratio of ~18 dB can be realized within device length of 30 μm.

By combining the mode converter and asymmetric Y-coupler, a TM_0 mode input is converted to TE_0 mode in the upper Y-branch and separated from TE_0 mode in the lower Y-branch evolved from the TE_0 mode input.

3. Simulated performance and fabrication tolerance

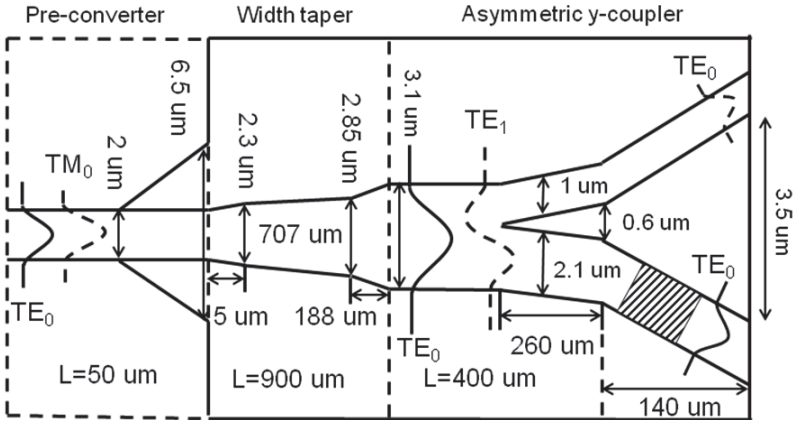

Fig. 5. The geometries of the mode-evolution-based polarization rotator-splitter after optimization.

Using the principle mentioned above, the device is designed and optimized. The commercial software Fimmwave employing eigenmode expansion method [19] is used for device optimization. The finite difference mode solver is used for solving modes in all sections. Figure 5 shows the geometries of the mode-evolution based polarization rotator-splitter after optimization. For the pre-converter, the length is 50 μm, the width for the higher level rib is 2 μm, and the width of the lower level rib varies from 2 μm to 6.5 μm. For the design of the lithography mask, the width of the lower level rib mask varies from 1 μm to 6.5 μm. This mask design will only require an accuracy of 0.5 μm to align the masks for two etch levels. A three-section width converter similar to the device in [12] is used in this work. The first section is 5 μm long and the width varies from 2 μm to 2.3 μm; the second section is 707 μm long and the width varies from 2.3 μm to 2.85 μm; the third section is 188 μm long and the width varies from 2.85 μm to 3.1 μm. A two-section asymmetric Y-coupler similar to the device in [20] is used in this work. For both sections, the upper branch waveguide is 1 μm wide and the lower branch waveguide is 2.1 μm wide. The first section is 260 μm long, and the separation between two branches varies from 0 μm to 0.6 μm; the second section is 140 μm long, and the separation between two branches varies from 0.6 μm to 3.5 μm. The integrated TE polarizer is 30 μm long. The total device length is 1350 μm. Sidewall scattering loss was not considered in the simulation, since it is expected to be small because of shallow etching. Waveguide absorption loss was also not included, since it is an independent parameter that can be optimized by the crystal growth.

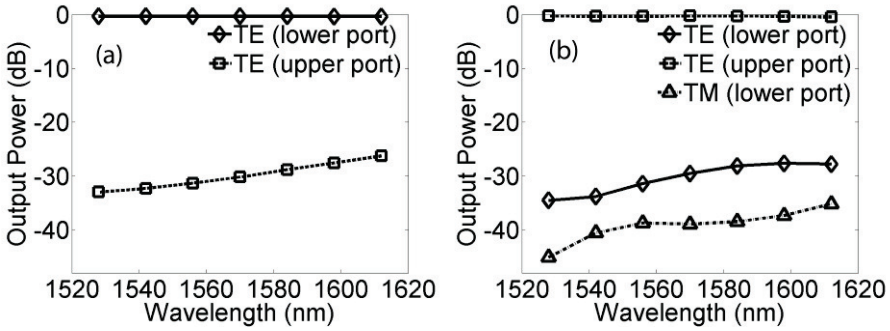

Fig. 6. The normalized TE_0 mode output power from the upper (diamond) and lower (square) Y-branches and the normalized TM_0 mode output power from the lower (triangle) Y-branch as function of wavelength excited by TE_0 mode input (a) and TM_0 mode input (b).

Figure 6 shows the normalized TE_0 mode output power from the upper and lower Y-branches and the normalized TM_0 mode output power from the lower Y-branches as a function of wavelength from 1528 nm to 1612 nm excited by TE_0 mode input (a) and TM_0 mode input (b). For TE_0 mode input, the device has an insertion loss below 0.37 dB and PER over 25 dB over the entire C (1528-1567 nm) +L (1565-1612 nm) band. For TM_0 mode input, the device has an insertion loss below 0.46 dB and PER over 27 dB over the entire C +L band.

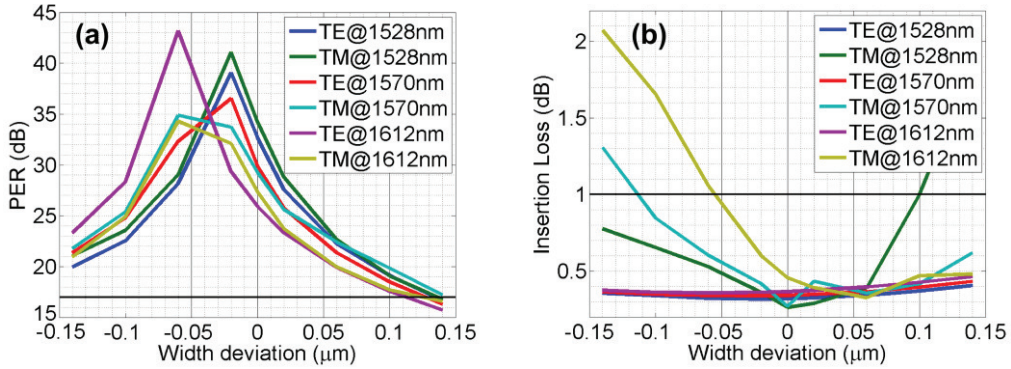

Fig. 7. (a) The PER and (b) the insertion loss of TE_0 and TM_0 modes at 1528 nm, 1570 nm, and 1612 nm.

Figure 7 shows (a) the PER and (b) the insertion loss of TE_0 and TM_0 modes at 1528 nm, 1570 nm, and 1612 nm, as a function of the waveguide width deviation from the design value. At the center wavelength of 1570 nm, for TE_0 mode input, the device has an insertion loss below 0.43 dB and PER over 17 dB with respect to a width variation of +/- 0.14 μm. For TM_0 mode, the device has an insertion loss below 1 dB and PER over 17 dB with respect to a width variation of +/- 0.12 μm. This compares favorably to the reported polarization splitter-rotator utilizing InGaAsP/InP structures, which have a fabrication tolerance of about +/- 0.05 μm for insertion loss less than 1 dB for TM_0 input [21]. To satisfy PER greater than 17 dB and insertion loss below 1 dB over the entire C+L band, the tolerance for the width is +/- 0.08 μm.

4. Conclusion

In this article, a mode-evolution-based polarization rotator-splitter is proposed by combining a mode converter and an adiabatic asymmetric Y-coupler. The mode converter consists of a bi-level taper and a width taper. A shallow etched structure is proposed for the width taper to enhance the polarization conversion efficiency. A TE polarizer integrated in the Y-coupler is proposed to enhance the polarization extinction ratio. The device has a total length of 1350 μm, a polarization extinction ratio over 25 dB and an insertion loss below 0.5 dB both for TE and TM modes, over the wavelength range from 1528 to 1612 nm, covering all C+L band. This device is easy to fabricate and only requires photolithography alignment of 0.5 μm. In addition, this device has a large fabrication tolerance. The insertion loss remains below 1 dB and the polarization extinction ratio remains over 17 dB with a width variation of +/- 0.12 μm at the wavelength of 1570 nm, or with a width variation of +/- 0.08 μm over the entire C+L band. Although this device is proposed and optimized for the InGaAsP/InP material system, it could also be employed for silicon on insulator or other material systems.